Template-based bias correction: Application to paediatric brain MRI

M. Murgasova[1], J. V. Hajnal[2], S. J. Counsell[2], A. D. Edwards[2], and D. Rueckert[1]

[1]Department of Computing, Imperial College London, London, United Kingdom, [2]Robert Steiner Magnetic Resonance Unit, Imaging Sciences Department, MRC Clinical Services Centre, Imperial College London, London, United Kingdom

INTRODUCTION

Inhomogeneity of the magnetic field during the acquisition of MR images results in a smooth variation of intensities within the image referred to as bias field. This artefact complicates not only the further processing of the images, such as tissue segmentation or registration, but also affects visual assessment if the intensity variation becomes very pronounced. Modern MR scanners operating at 3T or higher field strengths enable the acquisition of images with higher resolution at shorter scanning times. However, these images are also corrupted by stronger bias fields. Many standard bias correction methods (such as N3 [1]) are not effective in the presence of strong bias field. We propose a novel template-based bias correction method, which estimates the bias field by adjustment to an aligned and intensity-matched template image. Images acquired at lower magnetic field strength with a birdcage receiver coil with smaller bias fields can easily be corrected by more conventional means and therefore provide suitable templates. The method has been applied to 35 paediatric brain MR images with strong bias field, acquired on a 3T MR scanner.

METHOD

Subjects: T1-weighted MR images of 35 prematurely born children at the age of two years were acquired on a Phillips 3T scanner using a MP RAGE imaging sequence and reconstructed with voxel size 0.8 x 0.8 x 0.8 mm^3. T1-weighed MR image of a two year old subject acquired on a 1.0T HPQ system (Philips Medical Systems), reconstructed with voxels size 1.6 x 1.035 x 1.035 mm^3 was used as a template image, after bias correction using the N3 method [1].

Pre-processing: In the first stage the background voxels in each image were removed using tresholding followed by dilation, erosion and a region growing procedure. The template image was aligned with each subject using affine registration with normalized mutual information as a similarity measure [2]. A linear intensity transformation of the aligned templates was then performed to match intensity means and variances of the corresponding image.

Estimating the bias field: The multiplicative low-frequency model was exploited to estimate the bias field. A residual image was calculated as $r_i = \log(y_i / x_i)$, where r_i, x_i and y_i denote the intensities of voxels in residual image, template image and image to be corrected, respectively. As the bias field β has low-frequency characteristics, it can be modelled as 3D cubic tensor-product B-spline with control points D_j: $\beta_i = \sum_j D_j N_j(\mathbf{u}_i)$ where N_j denotes 3D cubic tensor-product B-spline basis function and $\mathbf{u}_i$ is the spatial location of the voxel β_i. The bias field was estimated by a least-square fit to the residual image: $\hat{\beta} = \arg\min_{\beta} \sum_i w_i (r_i - \beta_i)^2$. The influence of voxels with mismatched tissue content was reduced by assigning lower weights w_i. The weights and bias field were calculated iteratively: **1.** The residual image was bias corrected using the latest estimate of the bias field. A soft classification (a vector of posterior probabilities for each voxel, determining the probability of a voxel belonging to a tissue class) of the bias corrected residual image was calculated by fitting a mixture of two zero-mean Gaussians using the EM algorithm [3]: a Gaussian with small variance σ^2_{small} represented the voxels with the same tissue content and a Gaussian with large variance σ^2_{large} represented the mismatched voxels. **2.** The weights were calculated using the formula $w_i = p_{i,small} / \sigma^2_{small} + p_{i,large} / \sigma^2_{large}$ where $p_{i,small}$ and $p_{i,large}$ denotes the soft classification. **3.** The control points for the bias field can then be calculated from equation $N^T W N D = N^T W R$ using singular value decomposition [4]. Here the matrix N is composed of elements $N_{ij} = N_j(\mathbf{u}_i)$, W is a diagonal matrix of the weights w_i, R is a vector of intensities r_i and D is a vector of B-spline control points. The steps are repeated until convergence.

For the purposes of evaluation four images were segmented using EM segmentation [5] with a population-specific atlas [6] before and after bias correction with different B-spline control point spacings. The automatic segmentations were compared with manual segmentations on 7-8 slices including white matter and cortical grey matter using the Dice metric [7].

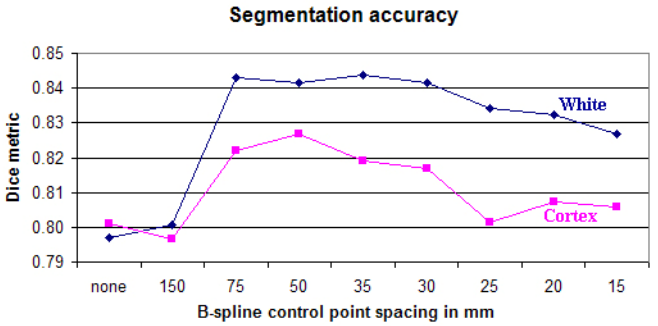

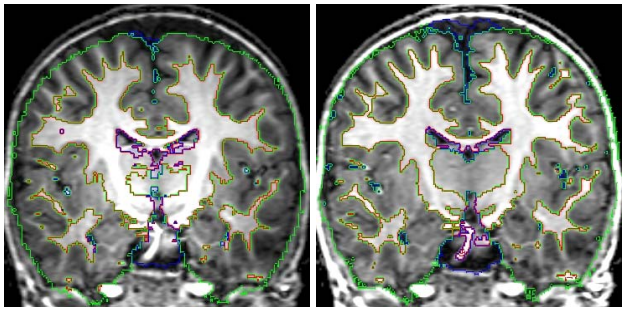

(a) **(b)**

RESULTS

The graph shows the agreement between manual and automated segmentation as a function of B-spline control point spacing. Control point spacing between 75 and 50mm produced the best results. A comparison of an original image (a) and the corresponding corrected image (b) with the segmentation result superimposed is shown on the right. The segmentation of the original image shows a distortion resulting from central brightening in the image caused by the bias field. The segmentation of the image corrected with the B-spline control point spacing 75mm shows considerable improvement.

CONCLUSION

We propose a template-based bias correction method based on weighted least-square B-spline fitting to estimate the bias field. We have shown that the method is highly effective on brain MRI with strong intensity inhomogeneity. The advantage of the method is its general applicability not only to MR images of the brain, but any organs for which a template image is available. In addition, the use of robust statistics in form of weighted least squares ensures that the method is robust to registration error. Only affine alignment is required to produce good results, which reduces computational demand, making the method efficient.

REFERENCES

1. Sled *et al.*: A nonparametric method for automatic correction of intensity non-uniformity in MRI data. *IEEE TMI*, 17(1):87–97, 1998. 2. Studholme *et al.*: An overlap invariant entropy measure of 3D medical image alignment. *Pattern Recognition*, 32(1):71–86, 1999. 3. Dempster *et al.*: Maximum likelihood from incomplete data via the EM-algorithm. *J. Royal Statistical Society*, 39(1):1–38, 1977. 4. Press *et al.*: *Numerical Recipes: The Art of Scientific Computing,* Cambridge University Press, 2007. 5. Van Leemput *et al.*: Automated model-based tissue classification of MR images of the brain. *IEEE TMI*, 18(10):897–908, 1999. 6. Murgasova *et al.*: Segmentation of brain MRI in young children. *Academic Radiology*, 14(11): 1350–66, 2007. 7. Dice: Measures of the amount of ecologic association between species. Ecology, 26:297–302, 1945.